EUROPEAN ORGANIZATION FOR NUCLEAR RESEARCH

CERN-OPEN-XX
19 August 1999

GEANT4 LOW ENERGY ELECTROMAGNETIC MODELS FOR ELECTRONS AND PHOTONS

J. Apostolakis[1], S. Giani[1], M. Maire[5], P. Nieminen[2], M.G. Pia[1,3], L. Urban[1,4]
[1]*CERN, CH-1211 Geneva 23, Switzerland*
[2]*ESA-ESTEC, Keplerlaan 1, 2200 AG Noordwjik, The Netherlands*
[3]*INFN, Sezione di Genova, I-16146 Genova, Italy*
[4]*RMKI Research Institute for Particle and Nuclear Physics, H-1525 Budapest, P.O.Box 49, Hungary*
[5]*LAPP, BP 110, F-74941, Annecy-le-Vieux*

Abstract

A set of physics processes has been developed in the Geant4 Simulation Toolkit to describe the electromagnetic interactions of photons and electrons with matter down to 250 eV. Preliminary comparisons of the models with experimental data show a satisfactory agreement.

1 Introduction

Geant4 [1] is a new-generation toolkit for full and fast Monte Carlo simulations, intended for a wide range of applications; these include high energy physics, space and cosmic ray simulations, nuclear and radiation analysis, and heavy ion and medical applications. Geant4 is based on the Object Oriented technology, has been developed using the C++ computer language, and provides the transparency of the physics implementation,

There are various grounds for differing specific requirements for these applications. In astrophysics, there is currently interest in conducting geological surveys of asteroids and other Solar System bodies by analysing the secondary X-ray line emissions from such bodies. These emissions can be induced either by natural sources (such as solar and galactic X-rays, cosmic rays, solar charged particles, trapped particles in planetary magnetospheres), or by artificial radioactive sources used in planetary or asteroid landers. On the other hand, space-borne X- and γ-ray astrophysical observatories experience undesirable background effects due to the space radiation environment. To determine the extent of these effects, Monte Carlo codes are often required. Other high energy physics applications - such as neutrino experiments - also have their specific requirements.

In medical applications, particularly in hadron irradiation treatment, the precise simulation of energy loss of both the incident particles and their secondary electrons in tissue is required, as is also analysis of the Bremsstrahlung process and the emission of fluorescence X-rays. Due to patient safety, accurate knowledge is required of the 3-D distribution of the absorbed radiation dose within small volumes, implying small step lengths in the simulation and consequently low energy thresholds. In the biological arena one can further distinguish the areas of microdosimetry and radiobiology, where the dimensions involved are even smaller, down to nanometre scale for cellular and DNA radiation damage studies.

The exact energy limit below which a Monte Carlo simulation in any of the above applications is discontinued is a trade-off between the accuracy required by the analysis, and the computer resources needed for the full transport. In most of the public domain electromagnetic codes, 1 keV is set as the ultimate cut-off energy. This limit has certain drawbacks. As can be seen in figure 1 [2]-[4], from diagnostic point of view 1 keV energy sets an elemental threshold (Z=11, or sodium) below which K-shell X-ray line emissions cannot be analysed. In astrophysical studies, for example, characteristic emissions from a number of common elements such as carbon, nitrogen or oxygen are consequently beyond the scope of the simulation.

To treat the various processes, codes having even higher cut-off energies (e.g. Geant3 at 10 keV) are often interfaced with one of the standard 1 keV-limit electromagnetic codes (like, for instance, EGS [5]). Apart from the added complexity for the end user, this option obviously is not ideal from the physics consistency and transparency point of view.

In Geant4, a set of models for the interactions of photons and electrons with matter - identified throughout this paper as Geant4 'standard' electromagnetic models [6] - is available, with the following lower energy limits:

- photoelectric effect: 10 keV,
- Compton effect: 10 keV,
- Rayleigh effect for optical photons,
- Bremsstrahlung: 1 keV,
- ionisation (discrete δ ray emission): 1 keV,
- multiple scattering: 1 keV.

In addition to the generation of secondaries, continuous energy loss along a tracking step is performed by the standard processes.

In this paper we report of a set of models that has been developed to describe the inter-

action of photons and electrons with matter at low energies [7]. These models are implemented in the Geant4 [1] toolkit, to extend the coverage of electromagnetic interactions down to 250 eV, a limit chosen to allow treatment of characteristic K-shell line emission down to Z=6 (carbon). The physics processes handled by these models include photoelectric effect, Compton scattering, Rayleigh effect, Bremsstrahlung and ionization.

2 Common features of Geant4 Low Energy electromagnetic processes

Some features common to all the Geant4 Low Energy processes are summarized in this section; more detailed information specific to each process is given in the following sections.

2.1 Generalities

The current models of the Geant4 Low Energy processes are valid for energies from 250 eV up to 100 GeV, unless differently specified in the following sections devoted to the detailed descriptions of each process. They cover elements with atomic number between 1 and 100.

All processes involve two distinct phases:

- the calculation of total cross sections,
- the generation of the final state.

Both phases are based on evaluated data from a set of data libraries: EADL (Evaluated Atomic Data Library) [8], EEDL (Evaluated Electrons Data Library) [9] and EPDL97 (Evaluated Photons Data Library) [10].

These libraries provide the following data relevant to the Geant4 Low Energy processes:

- total cross sections for photoelectric effect, Compton scattering, Rayleigh effect and Bremsstrahlung,
- subshell integrated cross sections for photoelectric effect and ionisation,
- energy spectra of the secondaries for electron processes,
- scattering functions for the Compton effect,
- form factors for the Rayleigh effect,
- binding energies for electrons for all subshells,
- transition probabilities between subshells for fluorescence and for the Auger effect.

The energy range covered by the data libraries extends from 100 GeV down to 1 eV for the Rayleigh and Compton effects, down to the lowest binding energy for each element for the photoelectric effect, down to 10 eV for Bremsstrahlung and down to the lowest subshell binding energy for each element for ionization.

The EADL, EEDL and EPDL97 data libraries are available from several public distribution centres [11]; a version of the libraries especially formatted for use with Geant4 is available from the Geant4 distribution source [12].

2.2 Calculation of total cross sections

The total cross sections as a function of energy are derived from the evaluated data for all the processes considered.

For each process the total cross section at a given energy E is obtained by interpolating the available data, according to the equation [14]:

$$\log(\sigma(E)) = log(\sigma_1)\frac{log(E_2) - log(E)}{log(E_2) - log(E_1)} + log(\sigma_2)\frac{log(E) - log(E_1)}{log(E_2) - log(E_1)} \qquad (1)$$

where E_1 and E_2 are the closest lower and higher energy for which cross section data σ_1 and σ_2 are available in the data libraries respectively.

In the case of ionization the partial cross sections for each subshell of an atom are first calculated at a given energy by interpolating the data according to equation 1, then the corresponding total cross section is obtained by summing the partial cross sections over all the shells.

2.3 Determination of the final state

The four-momenta of the final state products of the processes are determined according to distributions derived from the evaluated data.

The energy dependence of the parameters characterizing the sampling distributions is taken into account either by interpolation to the data available in the libraries directly or by interpolation to values obtained from fits to the data.

3 Compton scattering

The total cross section at a given energy E is calculated as described in section 2.2.

The scattered photon energy is distributed according to the product of the Klein-Nishina formula [16].

$$\Phi(\epsilon) \cong [\frac{1}{\epsilon} + \epsilon][1 - \frac{\epsilon sin^2(\theta)}{1+\epsilon^2}] \tag{2}$$

times the scattering functions $F(q)$:

$$P(\epsilon, q) = \Phi(\epsilon) \cdot F(q) \tag{3}$$

where ϵ is the ratio between the scattered photon energy and the incident photon energy. The scattering functions $F(q)$ at the transferred momentum $q = E \cdot \sin^2(\theta/2)$ corresponding to the energy E are calculated from the values available in the the EPDL97 data library. The angular distribution of the scattered photons is obtained from the same procedure.

The method applied for the sampling of the final state products according to the model described above is a combination of the composition and rejection Monte Carlo methods [17].

4 Rayleigh effect

The total cross section at a given energy E is calculated as described in section 2.2.

The angular distribution of the scattered photon is described by

$$\Phi(E, \theta) = [1 + cos^2(\theta)] \cdot F^2(q) \tag{4}$$

where $q = E \cdot sin^2(\theta/2)$ is the transferred momentum corresponding to energy E and $F(q)$ is the form factor. Form factors are obtained from the EPDL97 data libraries; their dependence on the momentum tranfer is taken into account by interpolating the available data.

5 Photoelectric effect

The total cross section at a given kinetic energy T is calculated as described in section 2.2.

The incident photon is absorbed and an electron of direction identical to the one of the incident photon is emitted. The subshell from which the electron is emitted is selected according to the cross sections of the subshells, determined as described in section 2.2.

The interaction leaves the atom in an excited state, with excitation energy equal to the binding energy of the subshell from which the electron has been emitted.

The deexcitation of the atom proceeds via the emission of fluorescence photons. The transition probabilities from a subshell to lower energy ones are extracted from the EADL data library. The fluorescence photons are generated with energy determined by the energy difference of the subshells involved in the transition and with isotropical distribution.

6 Bremsstrahlung

The total cross section at a given electron kinetic energy T is calculated as described in section 2.2.

The probability of the emission of a photon with kinetic energy t, considering an electron of incident energy T is generated according to:

$$Prob(T,t) = \frac{a(T)}{t} + b(T) \tag{5}$$

The energy distributions of the emitted photon available in the EEDL library for a few incident electron energies have been fitted to determine the values of the a and b coefficients at the corresponding incident energy; in the fits the Pearson χ^2 was utilized. The energy dependence of the a and b coefficients is then determined by a logarithmic interpolation for a and by a further fit for b.

The direction of the outcoming electron is the same as the direction of the incoming one.

The angular distribution of the emitted photons with respect to the incident electron is generated according to a simplified [17] formula based on Tsai cross section [18], which is expected to become isotropic in the low energy limit.

7 Ionisation

The total cross section at a given incident kinetic energy T is calculated by summing the partial cross sections at such energy for all the subshells of an element. The partial subshell cross sections at incident energy T are obtained from an interpolation of the evaluated cross section data in the EEDL library, according to the equation 1.

The subshell from which the electron is emitted is selected according to the values of the subshell cross sections, determined as described in section 2.2 from the EEDL library.

The probability of emission of an electron (δ ray) with kinetic energy t from a subshell of binding energy B_i as the result of the interaction of an incoming electron of kinetic energy T is described by:

$$Prob(T,t,B_i) = \sum_{j=2}^{7} \frac{a_j(T)}{(t+B_i)^j} \tag{6}$$

for $T < T_0$ and

$$Prob(T,t,B_i) = \frac{c(T)}{t^2} \tag{7}$$

for $T > T_0$, where T_0 is a parameter. Both formulas result from empirical fits to the EEDL data and are normalized to 1. The a and c coefficients are determined by fitting the data available at a set of discrete energies; their energy dependence is evaluated from a semilogarithmic interpolation of the values resulting from the fits.

The angle of emission of the scattered electron and of the δ ray is determined by energy-momentum conservation.

The interaction leaves the atom in an excited state, with excitation energy equal to the binding energy of the subshell from which the electron has been emitted. The deexcitation of the atom proceeds via the emission of fluorescence photons, as described in section 5.

8 Software implementation

The physics models described in this paper are implemented in the Geant4 Simulation Toolkit.

A comprehensive description of the Object Oriented design can be found in reference [15].

A lower energy limit for particle transport, corresponding to the minimal energy within the validity range of the models (250 eV), is defined. A higher threshold can be alternatively selected by the user of the Geant4 Toolkit, if this is desirable in any specific application. For a particle of energy E the mean free path for interacting via a given process is calculated as:

$$\lambda = \frac{1}{\Sigma_i \sigma_i(E) \cdot n_i} \tag{8}$$

where $\sigma_i(E)$ is the microscopic integrated cross section of the process considered at energy E and n_i is the atomic density number of the $i-th$ element contributing to the composition of the material where the interaction is occurring; the sum runs over all the elements the material is composed of. The cross sections are determined as described in section 2.2.

Particles with energy below the model validity range are assigned a zero mean free path; their energy is converted into a local energy deposit and they are not further tracked.

The final state is generated by sampling the relevant physics quantities (energies and angular distributions of the secondaries) according to the physics models described in the previous sections. The energy dependence of these distributions is taken into account by interpolating or fitting the available data.

The C++ code implementing the processes described in this paper is freely available from the Geant4 distribution source [12], together with its related software documentation [13].

9 Physics validation of the models

A set of comparisons between the predictions of the models described in this paper and experimental data has been performed. The results of the models described here have also been compared to the equivalent 'standard' electromagnetic models in the Geant4 Simulation Toolkit, at energies within the validity range of both sets of models; the Geant4 'standard' electromagnetic processes can be considered as a reference themselves, since they have been amply compared to experimental data [20]. The 'standard' processes produce results also in agreement with the EGS [5] Monte Carlo code. Figure 2 shows a good agreement between the distributions produced with Low Energy photon processes and the ones produced with Geant4 'standard' photon processes.

Figures 3 and 4 show the photon transmission resulting from Geant4 Low Energy models as a function of energy for 1 μm Al and Pb respectively: the simulation is in good agreement with experimental data [24]. The relevance of shell effects is clearly visible on the plots.

The physics performance of Low Energy ionization has been tested against experimental data reported in [22] and [23]. The energy distribution of 20 keV electrons transmitted through aluminum foils of 0.32 μm and 1 μm (figure 5) has been compared to the experimental data plotted in figure 6 of reference [22] and found to be in satisfactory agreement.

10 Conclusions

A set of models, based on the exploitation of evaluated data, has been developed to extend the coverage of electromagnetic interactions of photons and electrons down to 250 eV in the Geant4 Simulation Toolkit. The software implementing these models is freely available.

Preliminary comparisons of the models with experimental data show a good agreement.

Further extensions and refinements of the models described in this paper are planned by the Geant4 Collaboration in the future.

11 Acknowledgements

The authors wish to thank D. Cullen for kindly allowing the distribution of the EADL, EEDL and EPDL97 libraries with the Geant4 Simulation Toolkit and J. Stepanek for private

communications concerning the physics models.

References

[1] RD44 Collaboration, CERN/LHCC 98-44, LCB Status Report, 30 November 1998
[2] J.A. Bearden and A.F. Burr, Rev. Mod. Phys. **39** (1967) 125
[3] M. Cardona and L. Ley, Eds., Photoemission in Solids I. General Principles, Springer-Verlag, Berlin (1978)
[4] S. Kraft *et al.*, Rev. Sci. Instrum. **67** (1996) 681
[5] W.R. Nelson *et al.*, SLAC-R-265
[6] http://wwwinfo.cern.ch/asd/geant4/G4UsersDocuments/UsersGuides/ PhysicsReference-Manual/html/index.html
[7] J. Apostolakis, A. Forti, S. Giani, M. Maire, P. Nieminen, M.G. Pia, P. Truscott, L. Urban, Low-Energy Extension of Geant4 Electromagnetic Processes, To be published in the Proc. of the Space Radiation Environment Workshop, 1-3 November 1999, DERA, UK
[8] http://reddog1.llnl.gov/homepage.red/ATOMIC.htm
[9] http://reddog1.llnl.gov/homepage.red/Electron.htm
[10] http://reddog1.llnl.gov/homepage.red/photon.htm
[11] http://reddog1.llnl.gov/homepage.red/gowhere.htm
[12] http://wwwinfo.cern.ch/asd/geant4/source/source.html
[13] http://wwwinfo.cern.ch/asd/geant4/G4UsersDocuments/Overview/html/index.html
[14] J. Stepanek, New Photon, Positron and Electron Interaction Data for GEANT in Energy Range from 1 eV to 10 TeV, To be submitted for publication
[15] http://wwwinfo.cern.ch/asd/geant4/G4UsersDocuments/UsersGuides/ ForToolkitDeveloper/html/index.html
[16] O. Klein and Y. Nishina, Z. f. Physik **52** (1929), 853
[17] Geant3, CERN Program Library Long Writeup W5013
[18] Y.S. Tsai, Rev. Mod. Phys. **46** (1974) 815 and Rev. Mod. Phys. 49 (1977) 421
[19] Y. Kim and M.E. Rudd, Phys. Rev. **50** (1994) 3954
[20] http://wwwinfo.cern.ch/asd/geant4/reports/gallery/electromagnetic/
[21] http://wwwinfo.cern.ch/asd/geant/geant4_public/gallery/
[22] J. Baro *et al.*, NIM B **100** (1995) 31
[23] R. Shimizu *et al.*, J. Phys. D **9** (1976) 101.
[24] http://www.nsctoronto.com/joy_bs.html
[25] http://wwwinfo.cern.ch/asd/geant4/G4UsersDocuments/UsersGuides/ ForApplicationDeveloper/html/index.html

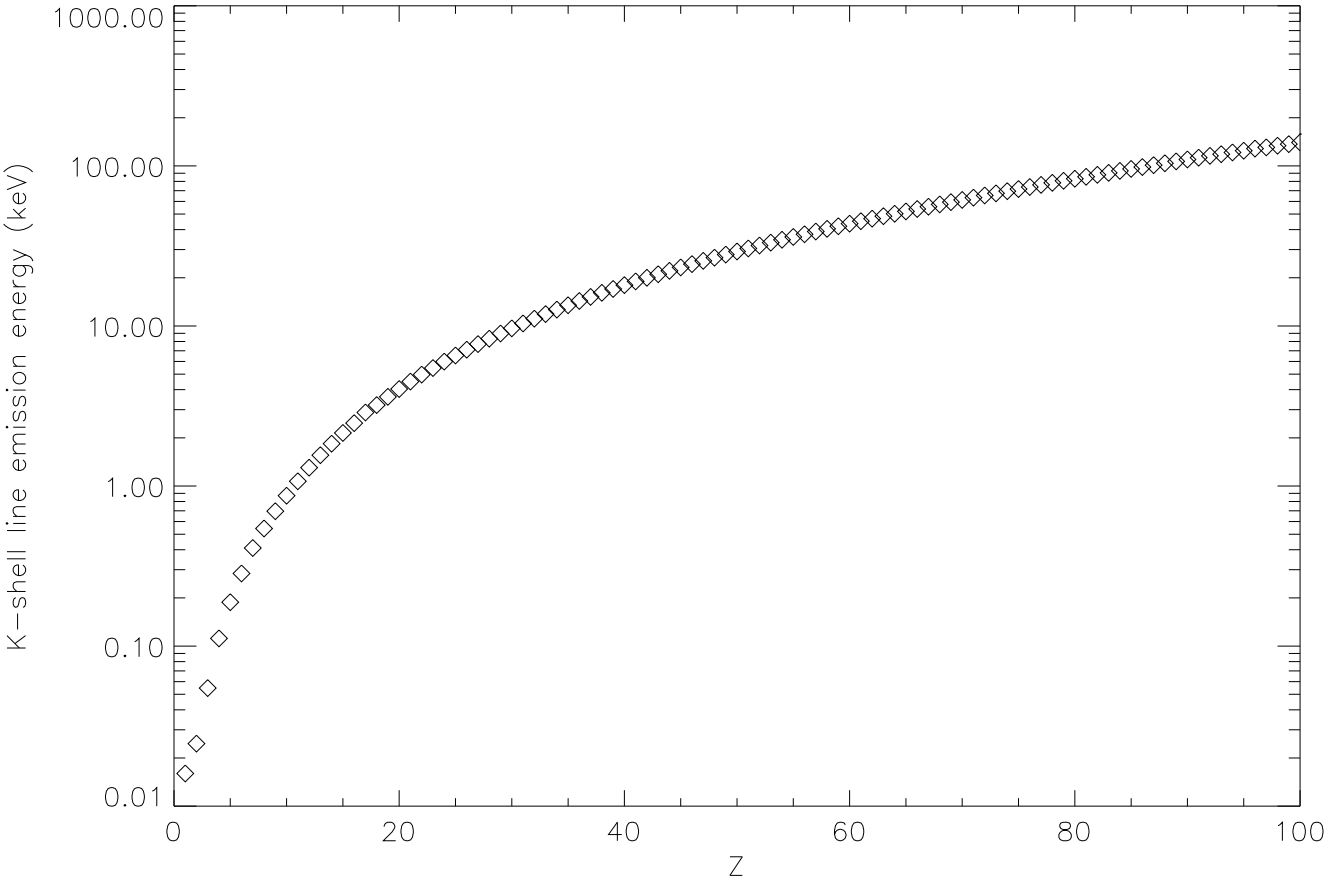

Figure 1: Principal K-shell X-ray line emission energy as a function of Z for elements Z=1 to 100.

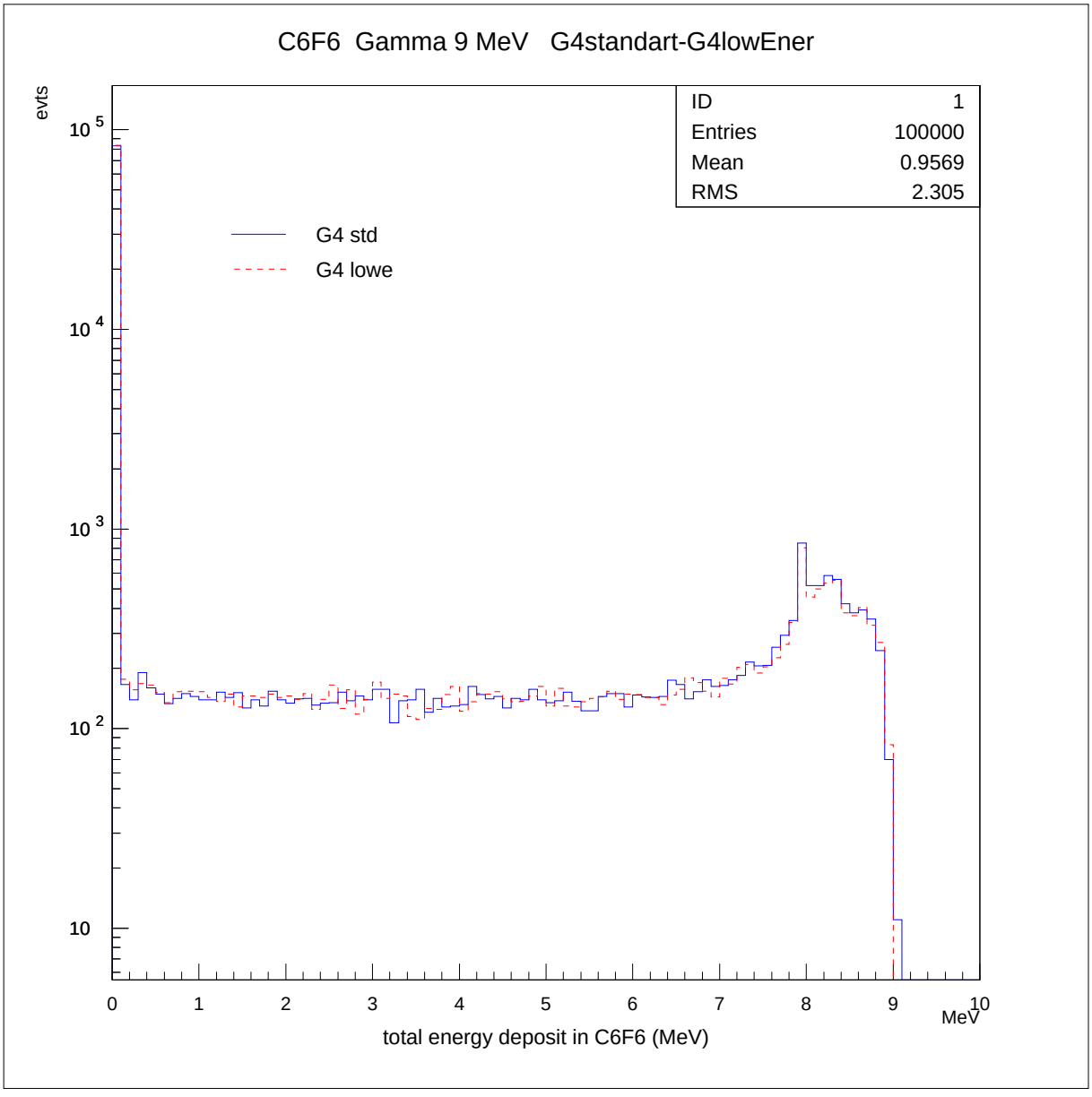

Figure 2: Comparison of standard and Low Energy photon processes: total energy deposit for 9 MeV photons in C_6F_6.

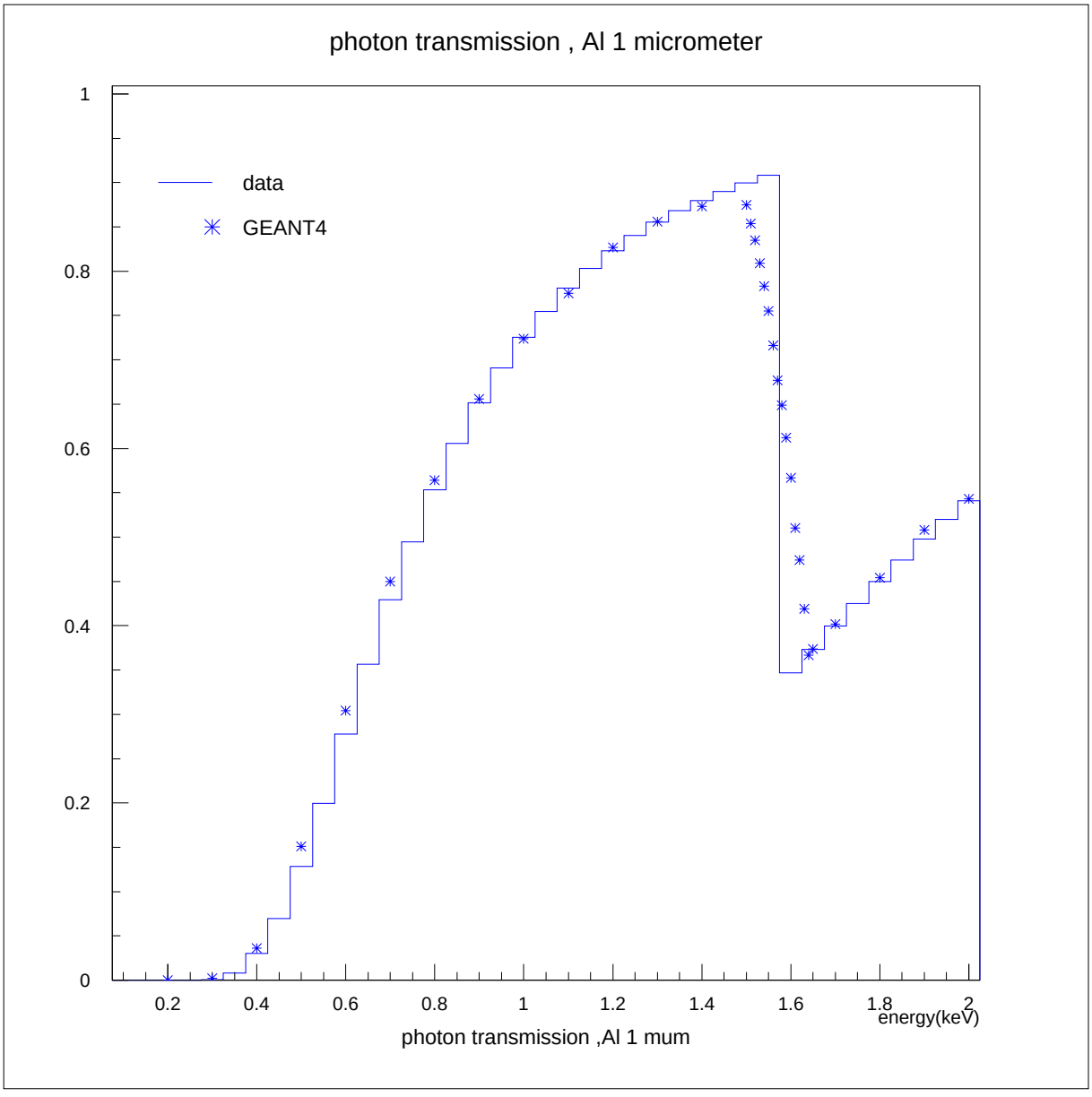

Figure 3: Comparison of the Geant4 Low Energy code and experimental data: photon transmission on 1 μm Al, with evidence of the relevance of shell effects.

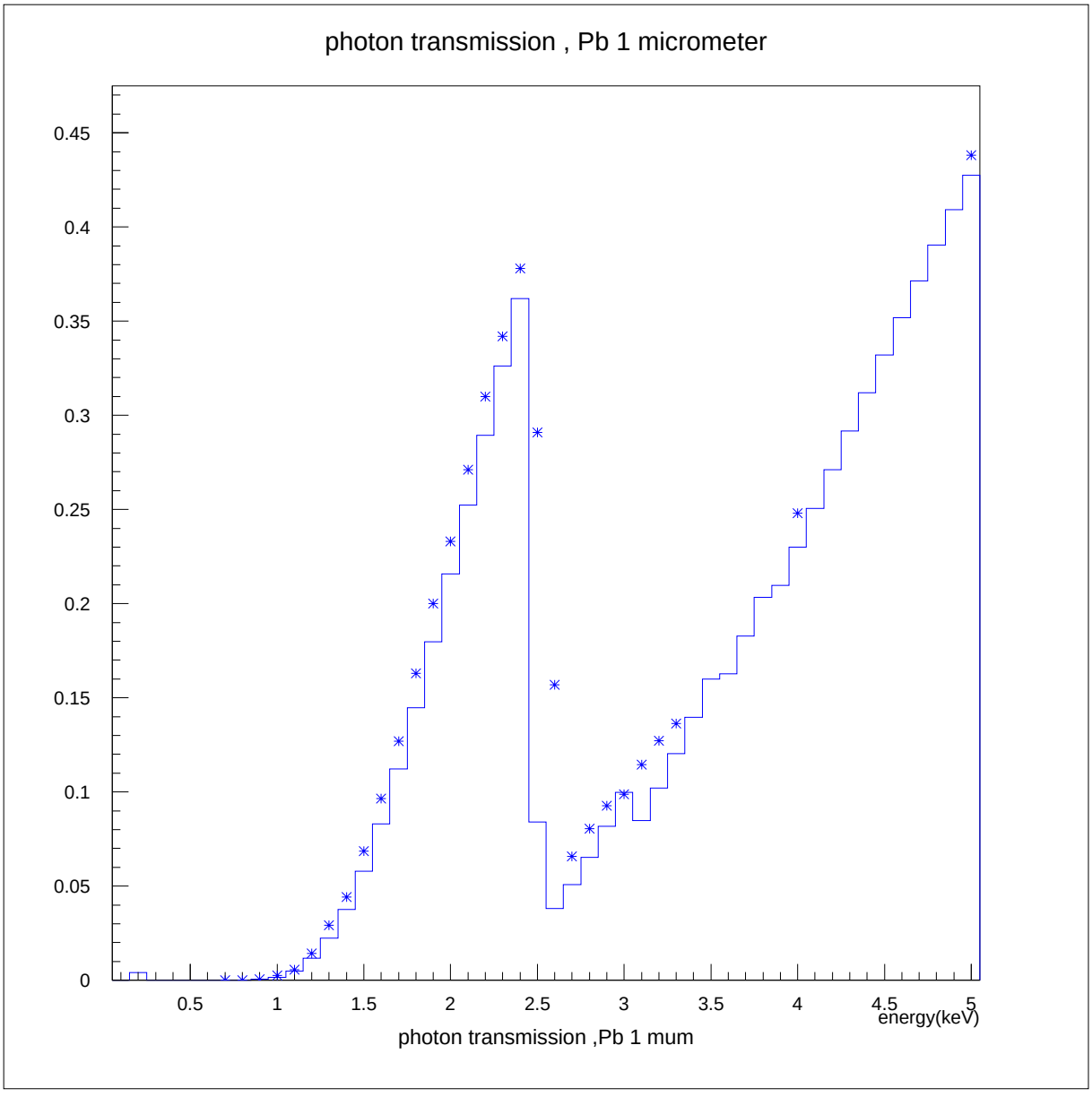

Figure 4: Comparison of the Geant4 Low Energy code and experimental data: photon transmission on 1 μm Pb, with evidence of the relevance of shell effects.

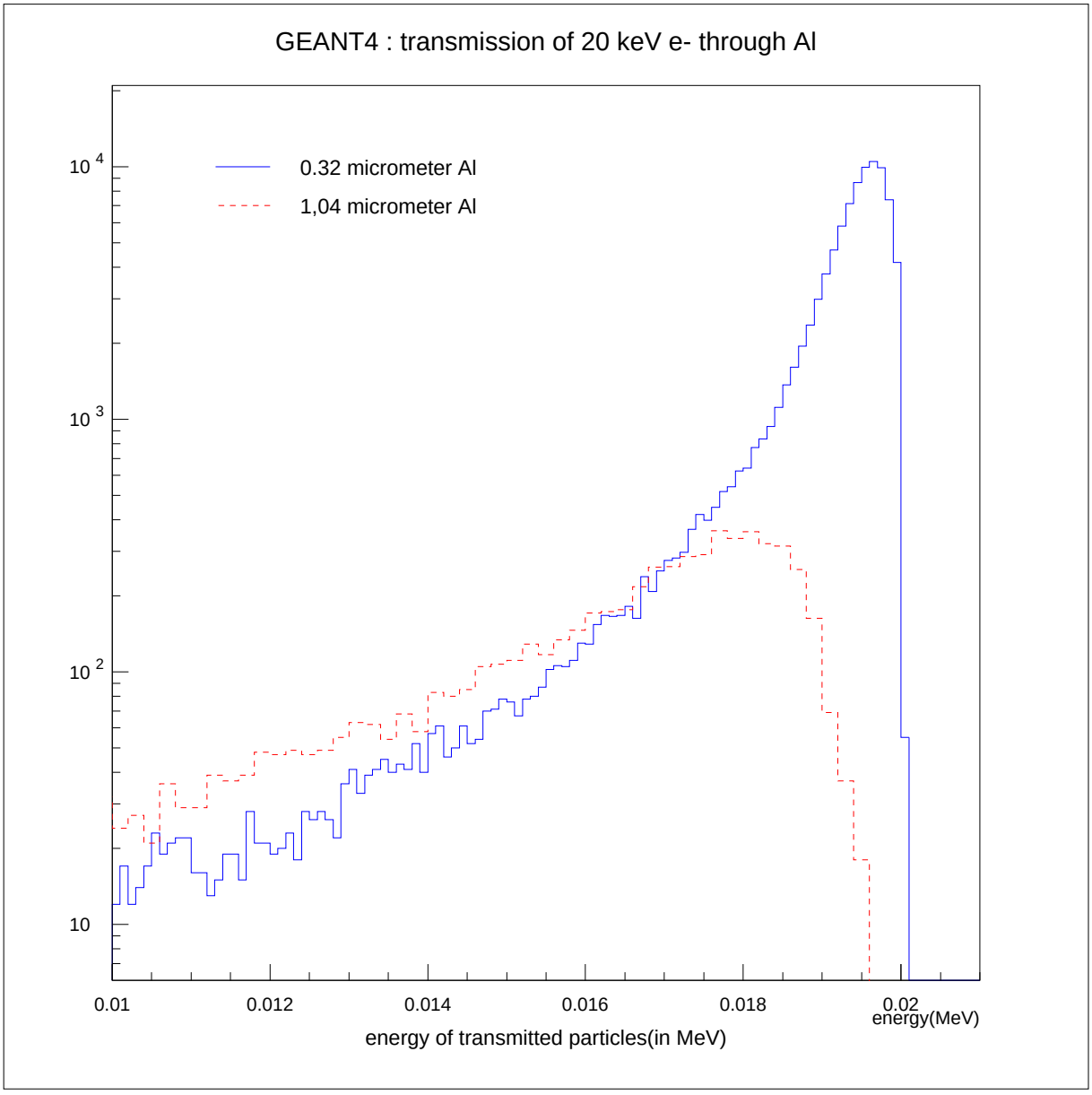

Figure 5: Comparison of the Geant4 Low Energy code and experimental data: energy of transmitted particles for 20 keV incident electrons, 1.04 μm and 0.32 μm Al, to be compared with figure 6 of reference [22].